Mesoporous Silica Nanoparticle Nanocarriers: Biofunctionality and Biocompatibility

DERRICK TARN,[‡] CARLEE E. ASHLEY,[||] MIN XUE,[‡]
ERIC C. CARNES,[§] JEFFREY I. ZINK,* AND C. JEFFREY BRINKER*, [§, ⊥, †]

[§]Department of Chemical and Nuclear Engineering and [⊥]Department of Molecular Genetics and Microbiology, the University of New Mexico, Albuquerque, New Mexico 87131, United States, [‡]Department of Chemistry and Biochemistry, University of California, Los Angeles, California 90095, United States, [||]Biotechnology and Bioengineering Department, Sandia National Laboratories, Livermore, California 94551, United States, and [†]Self-Assembled Materials Department, Sandia National Laboratories, Albuquerque, New Mexico 87185, United States

RECEIVED ON MARCH 30, 2012

CONSPECTUS

The study of ordered mesoporous silica materials has exploded since their discovery by Mobil researchers 20 years ago. The ability to make uniformly sized, porous, and dispersible nanoparticles using colloidal chemistry and evaporation-induced self-assembly has led to many applications of mesoporous silica nanoparticles (MSNPs) as "nanocarriers" for delivery of drugs and other cargos to cells. The exceptionally high surface area of MSNPs, often exceeding 1000 m^2/g, and the ability to independently modify pore size and surface chemistry, enables the loading of diverse cargos and cargo combinations at levels exceeding those of other common drug delivery carriers such as liposomes or polymer conjugates. This is because noncovalent electrostatic, hydrogen-bonding, and van der Waals interactions of the cargo with the MSNP internal surface cause preferential adsorption of cargo to the MSNP, allowing loading capacities to surpass the solubility limit of a solution or that achievable by osmotic gradient loading. The ability to independently modify the MSNP surface and interior makes possible engineered biofunctionality and biocompatibility.

In this Account, we detail our recent efforts to develop MSNPs as biocompatible nanocarriers (Figure 1) that simultaneously display multiple functions including (1) high visibility/contrast in multiple imaging modalities, (2) dispersibility, (3) binding specificity to a particular target tissue or cell type, (4) ability to load and deliver large concentrations of diverse cargos, and (5) triggered or controlled release of cargo. Toward function 1, we chemically conjugated fluorescent dyes or incorporated magnetic nanoparticles to enable *in vivo* optical or magnetic resonance imaging. For function 2, we have made MSNPs with polymer coatings, charged groups, or supported lipid bilayers, which decrease aggregation and improve stability in saline solutions. For functions 3 and 4, we have enhanced passive bioaccumulation via the enhanced permeability and retention effect by modifying the MSNP surfaces with positively charged polymers. We have also chemically attached ligands to MSNPs that selectively bind to receptors overexpressed in cancer cells. We have used encapsulation of MSNPs within reconfigurable supported lipid bilayers to develop new classes of responsive nanocarriers that actively interact with the target cell. Toward function 4, we exploit the high surface area and tailorable surface chemistry of MSNPs to retain hydrophobic drugs. Finally, for function 5, we have engineered dynamic behaviors by incorporating molecular machines within or at the entrances of MSNP pores and by using ligands, polymers, or lipid bilayers. These provide a means to seal-in and retain cargo and to direct MSNP interactions with and internalization by target cells.

Application of MSNPs as nanocarriers requires biocompatibility and low toxicity. Here the intrinsic porosity of the MSNP surface reduces the extent of hydrogen bonding or electrostatic interactions with cell membranes as does surface coating with polymers or lipid bilayers. Furthermore, the high surface area and low extent of condensation of the MSNP siloxane framework promote a high rate of dissolution into soluble silicic acid species, which are found to be nontoxic. Potential toxicity is further mitigated by the high drug capacity of MSNPs, which greatly reduces needed dosages compared with other nanocarriers. We anticipate that future generations of MSNPs incorporating molecular machines and encapsulated by membrane-like lipid bilayers will achieve a new level of controlled cellular interactions.
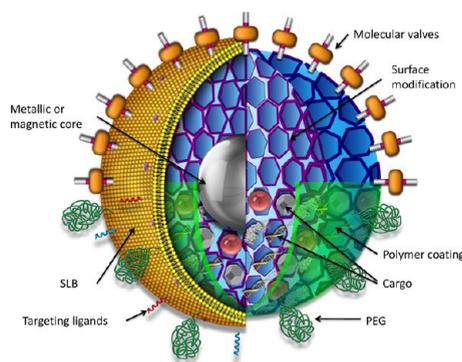
1. Introduction

History of Mesoporous Silica Nanoparticles (MSNPs). In their classic paper, Kresge and co-workers[1] described a means of combining sol−gel chemistry with liquid-crystalline templating to create new classes of ordered porous molecular sieves characterized by periodic arrangements of uniformly sized mesopores (defined by IUPAC as pores with diameters between 2 and 50 nm) incorporated within an amorphous silica matrix. Controlled synthesis of spherical and shaped mesoporous silica nanoparticles (MSNPs) has since been achieved by solution routes or by an aerosol-based evaporation-induced self-assembly[2] (EISA) process (Figure 2), and the pore surfaces have been modified with a wide range of chemical moieties based mainly on silane coupling chemistries. Now there exist MSNPs with varied internal and external surface chemistries and quite sophisticated, environmentally responsive characteristics including optical or pH modulation of molecular transport. This Account will review our recent efforts to develop biocompatible MSNPs with engineered functionalities and dynamic behaviors needed for the emerging field of nanoparticle-based drug delivery and diagnostics. A successful biocompatible nanocarrier must exhibit low toxicity combined with size uniformity, large capacity for diverse cargos, high traceability, colloidal stability, selective cell-specific binding and internalization, and triggered cargo release. We show how specific engineered chemical modifications of MSNPs result in functional and biocompatible nanocarriers (Figure 1). Both covalent modification and noncovalent encapsulation of MSNPs within polymers or supported lipid bilayers (SLB) enable nanocarrier imaging in both *in vitro* and *in vivo* systems, dispersion stability in biorelevant media, directed and cell-specific uptake and internalization, and high capacity loading and delivery of both hydrophilic and hydrophobic drugs.

2. Synthetic Routes to Mesoporous Silica

Solution-Based Synthesis of MSNPs. The most widely used type of MSNP is MCM-41, composed of ordered hexagonally arranged cylindrical mesopores.[1,3] Since its introduction by the Mobil company as micrometer-sized, amorphous aggregates, improved synthetic procedures enabled the formation of MCM-41 as successively smaller particles with controlled shape: submicrometer spheres,[4] 100−150 nm nanoparticles suitable for *in vitro* studies,[5] monodisperse 50−75 nm nanoparticles,[6] and recently, 25 nm MCM-41 like MSNPs.[7] The rapid progression of MCM-41 into a monodisperse, <100 nm size MSNP reflects the emerging demand for biocompatible, functional nanocarriers for biological applications.

The synthesis of MCM-41 involves liquid crystal templating using an alkylammonium salt, commonly cetyl trimethylammonium bromide (CTAB). In aqueous solution, above the critical micelle concentration, amphiphilic surfactant molecules self-assemble into spherical micelles and at higher concentrations into periodic liquid crystal mesophases. Conducted in the presence of water and hydrophilic, soluble silica precursors (e.g., silicic acid, $Si(OH)_4$, or polysilicic acids), surfactant self-assembly results in hybrid nanocomposites. Through electrostatic and hydrogen bonding interactions, the silica precursors are concentrated at hydrophilic interfaces and condense to form an amorphous silica mold of the ordered periodic mesophase. Subsequent removal of the surfactant template by extraction or calcination results in the mesoporous product.

Evaporation-Induced Self-Assembly (EISA). EISA was established in 1997 as a means to direct the formation of continuous thin film mesophases via dip-coating.[8] EISA starts with a homogeneous solution of soluble silica and surfactant in ethanol/water with an initial surfactant concentration of conc ≪ cmc. Solvent evaporation during dip-coating or any evaporative process[2,8−11] progressively increases surfactant concentration, driving self-assembly of silica/surfactant micelles and their further organization into liquid-crystalline mesophases. A logical extension of the EISA thin film process was to use aerosol processing to direct the formation of spherical mesoporous nanoparticles.[10] Compared with solution routes, a potential advantage of EISA is that any nonvolatile component that can be introduced into an aerosol droplet is inevitably incorporated within the MSNP, where the liquid-crystalline nature of the silica−surfactant mesophase allows the foreign object to be conformally encapsulated.

3. Methods of MSNP Modification

Chemical Modification. MSNP functionality can be introduced by modifying silanol groups present both within the pore interiors and on the outer surface. These groups are chemically accessible and can be easily reacted with alkoxysilane derivatives to introduce organic functionality. Chemical moieties can also be adsorbed onto MSNP, especially facilitated by negatively charged SiO^- groups, resulting from deprotonation of surface silanol groups at neutral pH, which result in attractive electrostatic interactions with positively charged mioeties (Figure 1). Generally, two main routes
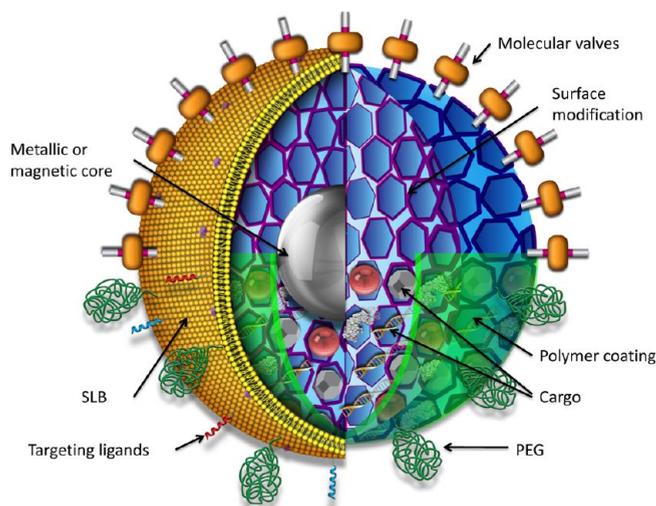
FIGURE 1. Schematic of a multifunctional mesoporous silica nanoparticle showing possible core/shell design, surface modifications, and multiple types of cargos.

of modification exist: co-condensation, and postsynthetic grafting.

Co-condensation. The co-condensation method involves co-condensing hydrolyzed alkoxysilanes with organoalkoxysilanes ($R'_xSi(OR)_{4-x}$), which results in a directed modification of the interior pore surface.[12] The amphiphilic nature of the hydrolyzed organosilane allows it to serve as a cosurfactant that is incorporated into the surfactant micelle. As silica is condensed, the organoalkoxysilane is co-condensed positioning the organic moiety directly onto the pore walls.

An extension of the co-condensation method is the synthesis of MSNPs surrounding metal or metal oxide nanoparticles in a core–shell architecture (Figure 2).[13] Core–shell MSNPs have seen many recent applications in theranostics. the combination of therapy and diagnostics.[14]

Postsynthetic Grafting. A second method, postsynthetic grafting, involves modification of MSNPs after synthesis. This method employs surface-accessible silanol groups both within the mesopore network and on the exterior MSNP surfaces. Maximal surface coverage of interior mesopores is achieved via condensation with trifunctional organosilanes $R'Si(OR)_3$ in an organic solvent and produces a self-assembled monolayer.[15] To restrict or bias the deposition to the exterior surface of the MSNP, the modification can be performed prior to extracting the templating agent. The templating agent can then be removed, and the protected, unreacted silanol groups in the pore interiors can be further modified. In this way, functionalization can be directed. The various types of MSNP modifications and their strategies for synthesis are summarized in Figure 3. With these strategies,

MSNPs can be engineered with functionalities to achieve specific biorelevant properties.

Surface Coating. Introducing functional groups on the MSNP exterior surface gives rise to additional surface properties. They can be further reacted as linkers to attach larger molecules or used to adsorb coatings through noncovalent interactions (Figures 1 and 4). For the latter case, polymers are commonly employed on MSNPs.[6,16−18] Due to the intrinsic negative charge of the silica surface resulting from deprotonation of surface silanols, bare nanoparticles can be electrostatically functionalized with a positively charged polymer. Polymers or other surface bound functional groups can also be used to retain cargo within the MSNP.

An alternative means of surface coating MSNP is by the fusion with phospholipid bilayers to form a construct referred to as a protocell (Figure 4).[19−21] The cryo-TEM image (Figure 4b) shows a mesoporous silica particle core prepared by EISA enveloped by a conformal, 4-nm thick supported lipid bilayer (SLB). The properties of the SLB can be varied widely using lipids with differing fluidities or melting transition temperatures and headgroup chemistries that dictate charge and chemical reactivity. Membrane-bound components like cholesterol and PEG can be introduced to control the fluidity and stability of the SLB, and it can be chemically conjugated with ligands to effect targeting and internalization (*vide infra*). As with polymer coatings, the SLB can serve to retain cargo introduced into the MSNP interior.

4. Modified MSNPs for Biological Applications

A burgeoning area of MSNP research has been their use as nanocarriers in biology.[28] Consequently, much of our present work has been directed toward tailoring MSNP properties in order to improve their biofunctionality and biocompatibility. To be effective and universally applicable, nanocarriers must *simultaneously* demonstrate multiple functions and characteristics including (1) ease of imaging, (2) dispersibility, (3) specificity, (4) ability to load and deliver large concentrations of diverse cargos, and (5) biocompatibility and low toxicity. Their inherent high surface area, versatile surface chemistry, and low toxicity confer to MSNPs the characteristics of an ideal nanocarrier platform.

Imaging. Direct imaging of MSNPs under biorelevant conditions can be used to follow biodistribution, cancer cell targeting efficiency, internalization pathways, cytotoxicity, and the progress of therapy. MSNPs are multifunctional in that the core can be loaded or derivatized with fluorescent dyes, quantum dots, and therapeutic agents. Fluorescein
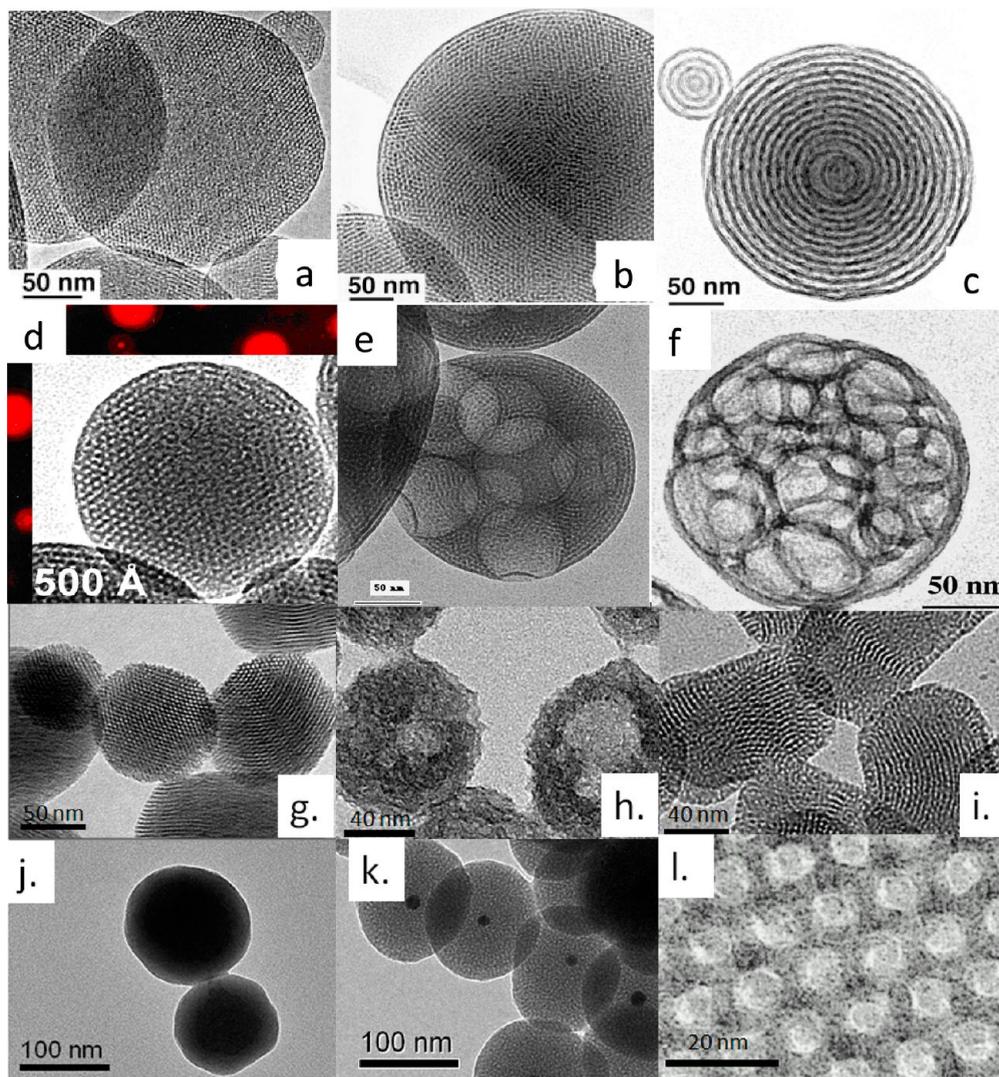
FIGURE 2. Gallery of mesoporous silica nanoparticles. Particles in panels a−d are formed by EISA. Lower panels are solution-prepared MSNPs.[7]

isothiocyanate (FITC) and rhodamine B isothiocyanate (RITC) are the most common fluorescent compounds that are incorporated into the MSNP core. Near-IR dyes, such as AlexaFluor 700 and DyLight 680, have also been used in MSNPs for imaging. This type of fluorescent labeling is fairly robust and can be easily achieved. The resulting fluorescent MSNPs are capable of generating high-resolution, multichannel images and can also provide quantitative data using flow cytometry techniques.[16] As an example, Figure 5a shows eight channel hyperspectral confocal images of four fluorescently labeled cargo classes delivered using targeted protocells. Colocalization of the cargo, silica, and lipid after 15 min is consistent with a receptor-mediated endocytotic pathway (Figure 6).[19] After 12 hours (Figure 5b), pH-triggered cargo release and endosomal disruption delivers the cargo into the cytosol.

Another relatively new method of imaging MSNPs is to incorporate magnetic nanoparticles, e.g., magnetite Fe_3O_4, as cores of the MSNPs, which allows T_2-weighted MRI imaging.[16] Alternatively, T_1-weighted imaging can be achieved using a chelated gadolinium compound.[22]

Dispersibility. For their use in biomedical applications, MSNPs must remain highly dispersed requiring colloidal stability. If aggregated, cell internalization suffers, biodistribution is difficult to control, and larger effective particle sizes may lead to potentially higher toxicity (see MSNP Toxicity). Particle agglomeration can be reduced by chemically modifying the surfaces,[23] introducing surface coatings with proteins or polymers,[6] and coating with a supported lipid bilayer.[19−21] These methods provide steric hindrance and electrostatic repulsion to achieve stable saline dispersions of MSNPs.
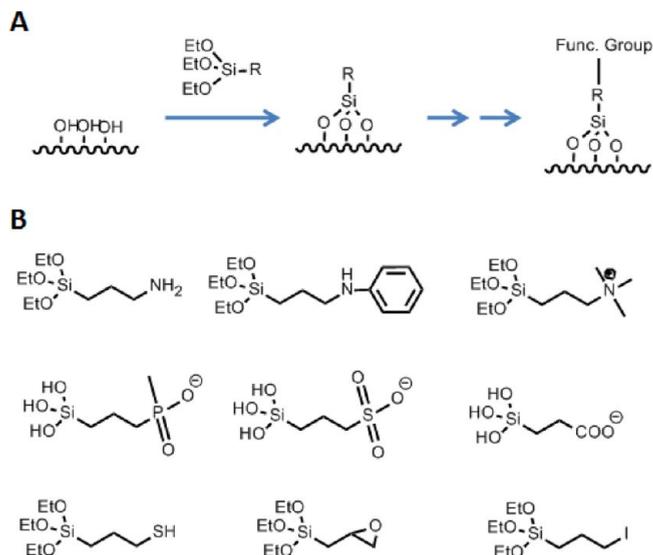
FIGURE 3. (a) Schematic showing reaction of surface silanol groups with an alkoxysilane linker to introduce functionality. (b) Various linkers to attach biomolecules or to change the surface properties.

Targeting Specificity. To limit the degree of nonspecific binding while enhancing specific internalization by the target cell or tissue, MSNPs can be actively targeted toward an intended region. Despite the success in developing MSNPs that passively accumulate at the site of interest, active targeting also plays an important role in enhancing overall bioavailability. Passive targeting schemes rely on the enhanced permeability of tumor vasculature (the so-called enhanced permeability and retention (EPR) effect[6] to direct accumulation of nanocarriers at tumor sites, but the lack of cell-specific interactions needed to induce nanocarrier internalization decreases therapeutic efficacy and can result in drug expulsion and induction of multiple drug resistance (MDR).[24] Selective targeting strategies employ ligands that specifically interact with receptors on the cell surface of interest to promote nanocarrier binding and internalization.[25] This strategy requires that receptors are highly overexpressed by cancer cells (10^4–10^5 copies/cell) relative to normal cells.
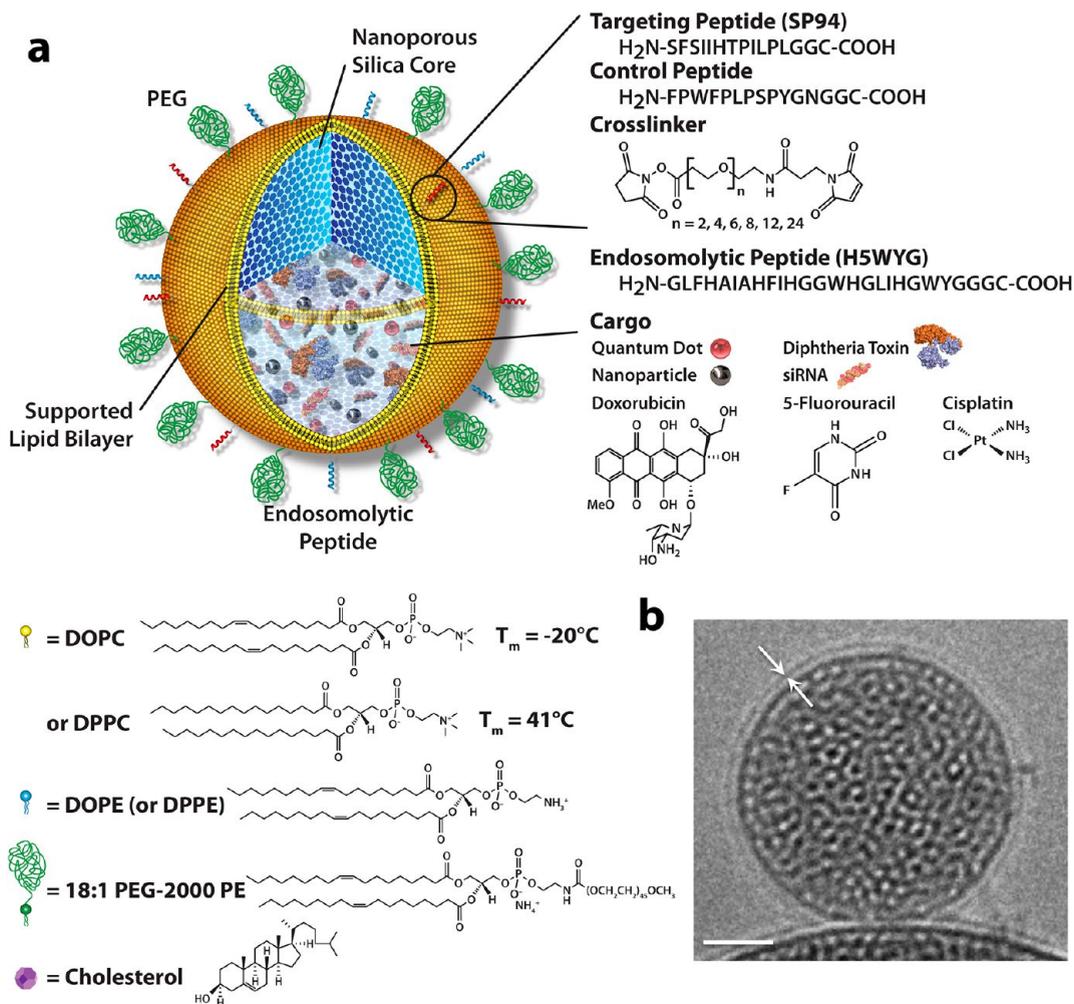
FIGURE 4. Schematic (a) and cryo-TEM image (b) of protocells. Adapted from ref 19.
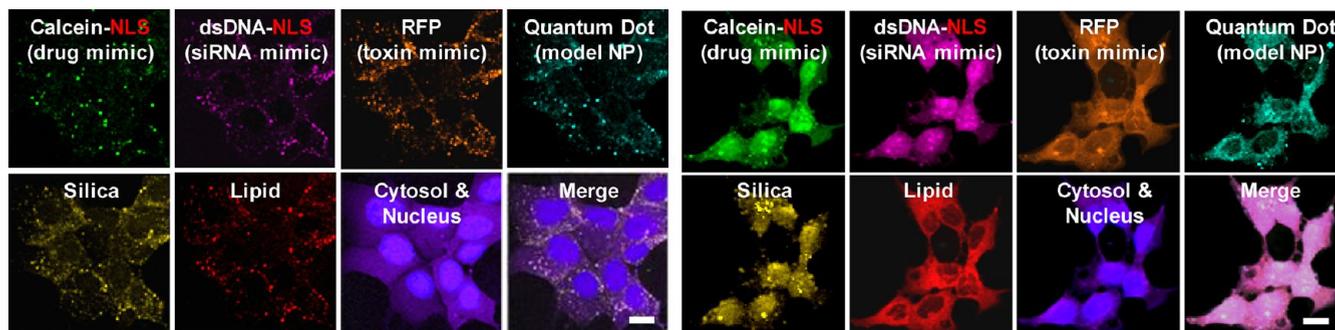
FIGURE 5. Hyperspectral confocal imaging of targeted delivery of multicomponent cargos in protocells to Hep3B cells for 15 minutes (left panel) or 12 hours (right panel) at 37 °C. Alexa Fluor 532-labeled nanoporous silica cores (yellow) were loaded with calcein (green), an Alexa Fluor 647-labeled dsDNA oligonucleotide (magenta), RFP (orange), and CdSe/ZnS quantum dots (teal). Cargos were sealed in the cores by fusion of Texas Red-labeled DOPC liposomes (red). Adapted from ref 17.
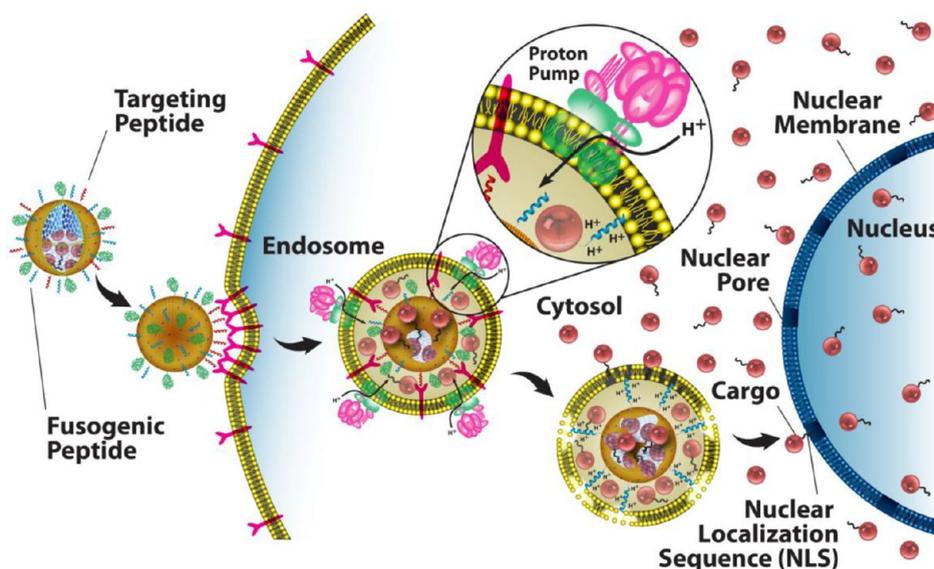
FIGURE 6. Schematic diagram depicting the successive steps of multivalent binding and internalization of targeted MSNP-supported lipid bilayers, followed by endosomal escape and nuclear localization of MSNP-encapsulated cargo. Adapted from ref 17.

In terms of passive targeting, Xia et al. demonstrated that cationic polymer (PEI) coating of MSNPs significantly facilitates their uptake.[17] Meng et al. showed that through combined size control and PEI/PEG copolymer coating, an enhanced EPR effect can be observed on a xenograft model.[6]

Active targeting employs ligands that bind specifically to receptors overexpressed on the cancer cell surface. Bioactive ligands, such as folate, RGD peptide, and transferrin have been employed[26] due to their respective receptors being overexpressed on many different cancer cell types. In general, high specificity and binding affinity require a high concentration of surface-conjugated ligands to promote multivalent binding effects, which result in more efficient drug delivery through receptor-mediated internalization pathways (Figure 6). However, high ligand densities can promote nonspecific interactions with endothelial and other noncancerous cells and

increase immunogenicity, resulting in opsonization-mediated clearance of nanocarriers. In this regard, the MSNP supported lipid bilayer construct (protocell) provides some potential advantages because its fluid SLB enables targeting ligand recruitment to target cell surface receptors, promoting high avidity with a low overall peptide concentration (Figure 7).

Cargo Loading and Delivery. The high surface area and controllable chemistry of the MSNPs allow for simple loading of high concentrations[12,19,20] of diverse classes and combination of cargos that can be delivered by endocytosis (Figure 6) or macropinocytosis. Early studies of drug delivery using MSNPs focused on drugs exhibiting low solubility in water, in particular, ibuprofen and aspirin.[27] Lu and Liong et al. later demonstrated the delivery of a hydrophobic chemotherapeutic agent, camptothecin, into cancer cells using MSNPs.[23] The high pore volume and surface area of MSNPs allows
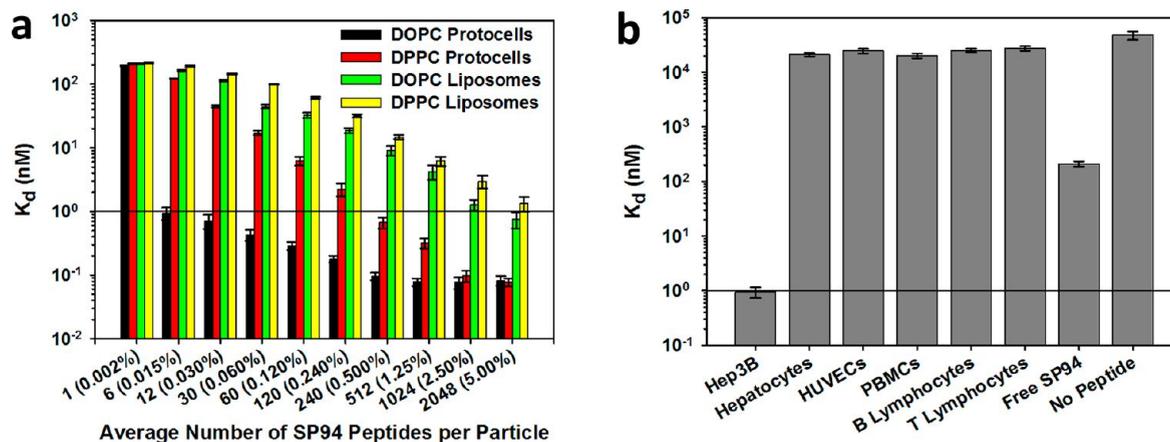
FIGURE 7. Selective and nonselective binding characteristics of peptide (SP94)-targeted protocells. (a) Dissociation constants (K_d) of SP94-targeted protocells and liposomes for the target hepatocarcinoma cell, Hep3B, as a function of the average number of SP94 peptides per particle (average SP94 wt % is in parentheses). (b) Dissociation constants (K_d) of SP94-targeted protocells for the target Hep3B and selected nontarget control cells. Peptide density is 0.015 wt %. All surface-binding experiments were conducted at 4 °C to prevent internalization of targeted protocells and liposomes. All error bars in panels a and b represent 95% confidence intervals (1.96σ) for $n = 5$. See ref 19 and Supporting Information therein.

hydrophobic compounds to be loaded into the pores from a nonaqueous solution and be retained in aqueous environments. When MSNPs are internalized through endocytosis (Figure 6), it is envisioned that lipid membrane components facilitate the phase transfer of the stored hydrophobic payload enabling it to be gradually released.

When a hydrophilic cargo is involved, further modification of the MSNPs is often required. Meng and Liong et al. attached negatively charged groups onto MSNPs to enable the loading and retention of the positively charged hydrophilic drug, doxorubicin (DOX).[18] Compared with FDA-approved Doxil, the doxorubicin capacity in MSNPs can be nearly 1000 times greater due to the high surface area and attractive electrostatic interactions.[19]

For most nanocarrier delivery strategies, the cargo must be retained within the nanocarrier and released only upon delivery to the target cell. For MSNPs, this generally requires that either the cargo be strongly adsorbed, as for DOX described above, or that the pores be "sealed" after cargo loading. A method where quantum dots and small nanoparticles (caps) were used to block the entrance of pores was developed.[28] Numerous strategies have been demonstrated where, by constructing a supramolecular nanovalve on the outer surface of MSNPs, one can achieve controlled release via a variety of stimuli, such as pH change, enzymatic ligand cleavage, light, and externally applied magnetic fields.[29−32] Polymer coatings[33] or supported lipid bilayers[19−21] have also been proven effective in sealing cargos within MSNPs, where in the latter case endosome-disrupting peptides were used to achieve pH-triggered cargo release into the cytosol.

5. Toxicity

MSNP Toxicity. A critical issue for any nanocarrier application is nanoparticle toxicity. The toxicity of silicon dioxide, both crystalline and amorphous, has been studied for more than a century, especially as it relates to silicosis,[34−37] and recently, the toxicity of silica nanoparticles has been extensively investigated, because the high surface to volume ratio of nanoparticles could lead to enhanced cellular interactions and different pathways of toxicity compared with coarse-grained silica.[6] Despite hundreds of studies of the toxicity of amorphous and crystalline silicas,[34−37] the mechanism(s) by which silica exposure leads to silicosis remains unclear, and literature reports are at times contradictory. Here it should be emphasized that *all silica is not created equal*. The amorphous silica framework and surface chemistry, in particular, hydroxyl coverage[38] and size and distribution of siloxane rings that comprise the framework structure,[39] can result in a wide range of configurations depending on processing conditions and environmental exposure. Consequently, there have been widely differing reports concerning the toxicity of MSNPs and amorphous silica in general.[7,40−42] There is, however, a general consensus that toxicity is associated in part with surface silanol ($\equiv$SiOH) groups,[43] which can hydrogen bond to membrane components[44] or when dissociated to form SiO$^-$ (above the isoelectric point of silica ∼pH 2−3), interact electrostatically with the positively charged tetraalkylammonium-containing phospholipids,[44] both processes leading to strong interactions and possibly membranolysis. Such a process occurring at the cell surface could cause lysis, for example, hemolysis, as shown for red blood cells.[7,42,44] Within a

phagosome, damage to the membrane could cause release of hydrolytic enzymes from lysosomes into the cytoplasm. In support of the importance of silanols, it is known that treating the silica surface with poly(vinylpyridine-*N*-oxide), aluminum salts, or surfactants can reduce or even switch-off hemolysis of red blood cells.[44] Based on the high surface to volume ratio of silica NPs, it might be anticipated that they would show in general higher toxicity compared with their bulk counterparts. However in the case of mesoporous silica NPs, the reduced solid fraction of the MSNP surface serves to reduce the surface area normalized hydroxyl coverage and therefore the extent of hydrogen bonding and electrostatic interactions between the MSNP and the cell membrane.[43] Additionally, based on membrane curvature arguments, very small NPs are less likely to disrupt or become internalized by the cell membrane[43] because the membrane binding energy needed for the cell membrane to contact and fully envelop the NP scales quadratically with the NP curvature (1/diameter).

A second contribution to toxicity can be the reaction of radicals present on the silica surface with water to yield reactive oxygen species (ROS), in particular, the hydroxy radical HO[•], one of the most reactive species in nature.[45] ROS can cause cell death by disrupting cell membranes (necrosis) or initiating programmed cell death (apoptosis). In sublethal concentrations, ROS can upregulate production of cytokines and other inflammatory mediators and can promote mutagenesis and carcinogenesis. Although the ability of freshly ground crystalline silicas to serve as generators of ROS is generally recognized and has been linked to traces of iron suggesting a Fenton-like mechanism, the ability of iron-free and amorphous silicas to generate ROS is just beginning to be appreciated.[46] Here it is noteworthy that depending on processing conditions, amorphous silicas can contain significant populations of strained three-membered siloxane rings.[47,39] Strained siloxane rings could undergo homolytic cleavage to form surface-associated radicals including the nonbridging oxygen hole center,[48] which react exothermically with water to form hydroxy radicals.[45] Whether, like defects generated by grinding of crystalline silica, strained three-membered rings in amorphous silica could serve as ROS generators is a question we are currently addressing.[39] Notably, as-synthesized and surfactant-extracted MSNPs have a negligible concentration of three-membered rings.[39] For amorphous silica nanoparticles in general, dissolution results in monosilicic acid or oligosilicic acid, which have been shown to have no intrinsic toxicity.[49]

Although based on numerous recent studies, it is generally observed that MSNPs have much lower toxicity than
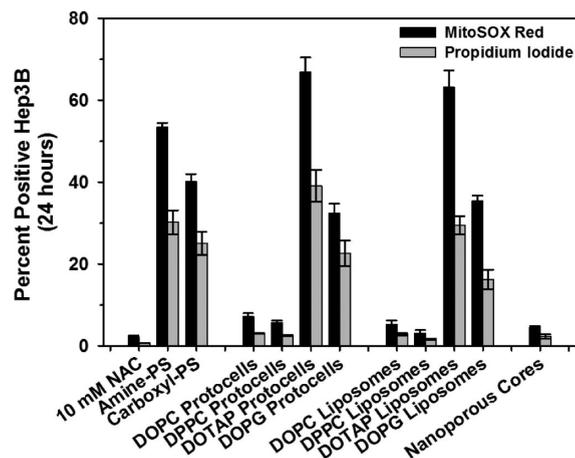
FIGURE 8. Reactive oxygen species generation (MitoSox Red) and % cell death (propidium iodide) of Hep3B cells exposed at 37 °C to MSNPs (nanoporous core), neutral, cationic, or anionic (DOTAP or DOPG) protocells, liposomes, and polystyrene beads for 24 hours. The antioxidant *N*-acetylcysteine (NAC) was used as a negative control. (C. E. Ashley, unpublished data).

corresponding nonporous silica colloids (Stöber silica or LUDOX), presumably due to the mesoporosity reducing the effective MSNP/membrane contact area; conclusions concerning the role of particle size, shape, and charge are mixed. Notably Slowing et al.[43] report reduced hemolysis of red blood cells, whereas Lin and Haynes[7] report increased hemolysis with decreasing MSNP sizes over the range 25−260 nm diameters. Toxicity effects are also reported to be highly cell specific. Yu et al.[42] show RAW264.7 macrophage cells to be more sensitive to ∼115 nm solid or MSNPs than A549 cells, especially at very high doses of 250−500 μg/mL, and that solid Stöber silica colloids were more toxic and taken up into macrophage cells to a much greater extent than the corresponding MSNPs. Rationalization and unification of these varied findings requires a detailed understanding of possible internalization pathways. For endocytosis, membrane curvature arguments discussed above indicate that individual 50−60 nm diameter NPs should be most efficiently internalized as shown experimentally for targeted MSNPs.[19] Using spherical and rod-shaped MSNPs, Meng et al.[50] showed for HeLa and A549 cells that particle shape (aspect ratio) is actively sensed and can stimulate efficient NP uptake by macropinocytosis in which multiple NPs are incorporated at once within pinosomes. Toxicity associated with both membrane damage and the fate of endocytosed or pinocytosed MSNPs must be clearly established, and the role of NP aggregation on effective particle shape and membrane association or internalization must be elucidated. In an effort to benchmark MSNP toxicity against control NPs, Figure 8 compares oxidative stress and cell viability

of Hep3B cells exposed to bare MSNPs with neutral, positively, and negatively charged MSNP-supported lipid bilayers, liposomes, and polystyrene NPs at 10^9 particles/mL corresponding to $\sim 1-2$ μg/mL. A trend of cationic > anionic > neutral NPs is observed, where cationic NPs in general are shown to have high ROS-associated toxicity.

The relevance of many recent MSNP toxicity studies to *in vivo* applications of MSNPs may be questionable however because coating the MSNPs with polymers, lipid bilayers, or proteins (as could immediately occur *in vivo*) screens electrostatic interactions with surface silanols and is observed to effectively eliminate toxicity as demonstrated *in vivo*.[51] Additionally when considering drug delivery, we must bear in mind potential therapeutically administered doses. For example, for the hepatocellular carcinoma cell line Hep3B, the LC_{50} and LC_{90} values of free DOX are 150 ng/mL and 500 ng/mL, respectively. Those quantities could be delivered in 400 ng/mL and 1.3 ug/mL of MSNPs. As shown by Ashley et al.,[19] when using targeted MSNPs, these values fall to 6 ng/mL and 20 ng/mL due to the MSNP capacity, stability, and internalization efficiency. If only a few percent of MSNP are delivered to the tumor microenvironment, relevant concentrations for the study of MSNP toxicity are less than about 100 μg/mL, where most studies have shown insignificant toxicity.

6. Future Directions

The multifunctional modular design of MSNPs shown in Figure 1 suggests next generation nanocarriers where multicomponent cargos are delivered to target cells through the active recruitment of targeting ligands combined with biologically triggered responses that actuate molecular valves. The combination of molecular machines and increasingly complex and biomimetic SLBs, for example, those derived from red blood cells,[52] may allow unprecedented engineering of NP/cellular interactions and provide a universal platform for theranostics and personalized medicine.

BIOGRAPHICAL INFORMATION

Derrick Tarn graduated in 2008 with a B.Sc. in Chemistry from UCLA. Currently, he is pursuing his Ph.D. under the supervision of Prof. Jeffrey I. Zink at UCLA, where his research is focused on the design and synthesis of nanomachines that function on both meso- and microporous silica nanoparticles.

Carlee E. Ashley graduated from UNM with a Ph.D. in chemical engineering in 2010 and is now a Truman Post-Doctoral Fellow at Sandia National Laboratories. Her work focuses on the development of targeted protocells and virus-like particles for applications in infectious disease and cancer therapy.

Min Xue graduated in 2008 from Nanjing University with a B.S. in Physical Chemistry. He is now pursuing his Ph.D. under the supervision of Prof. Jeffrey I. Zink at UCLA. Currently his research focus is on silica nanoparticle based drug delivery systems.

Eric C. Carnes graduated from UNM with a Ph.D. in chemical engineering in 2008 and is now a member of the technical staff at Sandia National Laboratories, where he studies the engineering of bio−nano interfaces for controlling cellular behavior and for development of targeted nanoparticle based drug delivery.

Jeffrey I. Zink is a Distinguished Professor of Chemistry at UCLA. He received his Ph.D. degree from the University of Illinois at Urbana−Champaign. His research interests include excited state properties of metal-containing molecules and multifunctional mechanized nanomaterials.

C. Jeffrey Brinker is a Fellow at Sandia National Laboratories and Distinguished Professor of Chemical Engineering at UNM, where he studies nanoscale materials made by self-assembly and directed assembly.

REFERENCES
1 Kresge, C. T.; Leonowicz, M. E.; Roth, W. J.; Vartuli, J. C.; Beck, J. S. Ordered mesoporous molecular sieves synthesized by a liquid-crystal template mechanism. *Nature* **1992**, *359*, 710–712.
2 Brinker, C. J.; Lu, Y. F.; Sellinger, A.; Fan, H. Y. Evaporation-induced self-assembly: Nanostructures made easy. *Adv. Mater.* **1999**, *11*, 579–585.
3 Beck, J. S.; Vartuli, J. C.; Roth, W. J.; Leonowicz, M. E.; Kresge, C. T.; Schmitt, K. D.; Chu, C. T. W.; Olson, D. H.; Sheppard, E. W. A new family of mesoporous molecular sieves prepared with liquid crystal templates. *J. Am. Chem. Soc.* **1992**, *114*, 10834–10843.

4 Grün, M.; Lauer, I.; Unger, K. K. The synthesis of micrometer- and submicrometer-size spheres of ordered mesoporous oxide MCM-41. *Adv. Mater.* **1997**, *9*, 254–257.

5 Huh, S.; Wiench, J. W.; Yoo, J.-C.; Pruski, M.; Lin, V. S. Y. Organic functionalization and morphology control of mesoporous silicas via a co-condensation synthesis method. *Chem. Mater.* **2003**, *15*, 4247–4256.

6 Meng, H.; Xue, M.; Xia, T.; Ji, Z.; Tarn, D. Y.; Zink, J. I.; Nel, A. E. Use of size and a copolymer design feature to improve the biodistribution and the enhanced permeability and retention effect of doxorubicin-loaded mesoporous silica nanoparticles in a murine xenograft tumor model. *ACS Nano* **2011**, *5*, 4131–4144.

7 Lin, Y.-S.; Haynes, C. L. Impacts of mesoporous silica nanoparticle size, pore ordering, and pore integrity on hemolytic activity. *J. Am. Chem. Soc.* **2010**, *132*, 4834–4842.

8 Lu, Y. F.; Ganguli, R.; Drewien, C. A.; Anderson, M. T.; Brinker, C. J.; Gong, W. L.; Guo, Y. X.; Soyez, H.; Dunn, B.; Huang, M. H.; Zink, J. I. Continuous formation of supported cubic and hexagonal mesoporous films by sol gel dip-coating. *Nature* **1997**, *389*, 364–368.

9 Huang, M. H.; Dunn, B. S.; Zink, J. I. In situ luminescence probing of the chemical and structural changes during formation of dip-coated lamellar phase sodium dodecyl sulfate sol—gel thin films. *J. Am. Chem. Soc.* **2000**, *122*, 3739–3745.

10 Lu, Y. F.; Fan, H. Y.; Stump, A.; Ward, T. L.; Rieker, T.; Brinker, C. J. Aerosol-assisted self-assembly of mesostructured spherical nanoparticles. *Nature* **1999**, *398*, 223–226.

11 Fan, H. Y.; Lu, Y. F.; Stump, A.; Reed, S. T.; Baer, T.; Schunk, R.; Perez-Luna, V.; Lopez, G. P.; Brinker, C. J. Rapid prototyping of patterned functional nanostructures. *Nature* **2000**, *405*, 56–60.

12 Li, Z.; Nyalosaso, J. L.; Hwang, A. A.; Ferris, D. P.; Yang, S.; Derrien, G.; Charnay, C.; Durand, J.-O.; Zink, J. I. Measurement of uptake and release capacities of mesoporous silica nanoparticles enabled by nanovalve gates. *J. Phys. Chem. C* **2011**, *115*, 19496–19506.

13 Kim, J.; Kim, H. S.; Lee, N.; Kim, T.; Kim, H.; Yu, T.; Song, I. C.; Moon, W. K.; Hyeon, T. Multifunctional uniform nanoparticles composed of a magnetite nanocrystal core and a mesoporous silica shell for magnetic resonance and fluorescence imaging and for drug delivery. *Angew. Chem., Int. Ed.* **2008**, *47*, 8438–8441.

14 Thomas, C. R.; Ferris, D. P.; Lee, J.-H.; Choi, E.; Cho, M. H.; Kim, E. S.; Stoddart, J. F.; Shin, J.-S.; Cheon, J.; Zink, J. I. Noninvasive remote-controlled release of drug molecules in vitro using magnetic actuation of mechanized nanoparticles. *J. Am. Chem. Soc.* **2010**, *132*, 10623–10625.

15 Feng, X.; Fryxell, G. E.; Wang, L.-Q.; Kim, A. Y.; Liu, J.; Kemner, K. M. Functionalized monolayers on ordered mesoporous supports. *Science* **1997**, *276*, 923–926.

16 Liong, M.; Lu, J.; Kovochich, M.; Xia, T.; Ruehm, S. G.; Nel, A. E.; Tamanoi, F.; Zink, J. I. Multifunctional inorganic nanoparticles for imaging, targeting, and drug delivery. *ACS Nano* **2008**, *2*, 889–896.

17 Xia, T.; Kovochich, M.; Liong, M.; Meng, H.; Kabehie, S.; George, S.; Zink, J. I.; Nel, A. E. Polyethyleneimine coating enhances the cellular uptake of mesoporous silica nanoparticles and allows safe delivery of siRNA and DNA constructs. *ACS Nano* **2009**, *3*, 3273–3286.

18 Meng, H.; Liong, M.; Xia, T.; Li, Z.; Ji, Z.; Zink, J. I.; Nel, A. E. Engineered design of mesoporous silica nanoparticles to deliver doxorubicin and P-glycoprotein siRNA to overcome drug resistance in a cancer cell line. *ACS Nano* **2010**, *4*, 4539–4550.

19 Ashley, C. E.; Carnes, E. C.; Phillips, G. K.; Padilla, D.; Durfee, P. N.; Brown, P. A.; Hanna, T. N.; Liu, J.; Phillips, B.; Carter, M. B.; Carroll, N. J.; Jiang, X.; Dunphy, D. R.; Willman, C. L.; Petsev, D. N.; Evans, D. G.; Parikh, A. N.; Chackerian, B.; Wharton, W.; Peabody, D. S.; Brinker, C. J. The targeted delivery of multicomponent cargos to cancer cells by nanoporous particle-supported lipid bilayers. *Nat. Mater.* **2011**, *10*, 389–397.

20 Ashley, C. E.; Carnes, E. C.; Epler, K. E.; Padilla, D. P.; Phillips, G. K.; Castillo, R. E.; Wilkinson, D. C.; Wilkinson, B. S.; Burgard, C. A.; Kalinich, R. M.; Townson, J. L.; Chackerian, B.; Willman, C. L.; Peabody, D. S.; Wharton, W.; Brinker, C. J. Delivery of small interfering RNA by peptide-targeted mesoporous silica nanoparticle-supported lipid bilayers. *ACS Nano* **2012**, *6*, 2174–2188.

21 Liu, J. W.; Stace-Naughton, A.; Jiang, X. M.; Brinker, C. J. Porous nanoparticle supported lipid bilayers (protocells) as delivery vehicles. *J. Am. Chem. Soc.* **2009**, *131*, 1354–1355.

22 Hsiao, J.-K.; Tsai, C.-P.; Chung, T.-H.; Hung, Y.; Yao, M.; Liu, H.-M.; Mou, C.-Y.; Yang, C.-S.; Chen, Y.-C.; Huang, D.-M. Mesoporous silica nanoparticles as a delivery system of gadolinium for effective human stem cell tracking. *Small* **2008**, *4*, 1445–1452.

23 Lu, J.; Liong, M.; Zink, J. I.; Tamanoi, F. Mesoporous silica nanoparticles as a delivery system for hydrophobic anticancer drugs. *Small* **2007**, *3*, 1341–1346.

24 Gottesman, M. M.; Fojo, T.; Bates, S. E. Multidrug resistance in cancer: Role of ATP-dependent transporters. *Nat. Rev. Cancer* **2002**, *2*, 48–58.

25 Sapra, P.; Allen, T. M. Internalizing antibodies are necessary for improved therapeutic efficacy of antibody-targeted liposomal drugs. *Cancer Res.* **2002**, *62*, 7190–7194.

26 Ferris, D. P.; Lu, J.; Gothard, C.; Yanes, R.; Thomas, C. R.; Olsen, J.-C.; Stoddart, J. F.; Tamanoi, F.; Zink, J. I. Synthesis of biomolecule-modified mesoporous silica nanoparticles for targeted hydrophobic drug delivery to cancer cells. *Small* **2011**, *7*, 1816–1826.

27 Vallet-Regi, M.; Rámila, A.; del Real, R. P.; Pérez-Pariente, J. A new property of MCM-41: Drug delivery system. *Chem. Mater.* **2001**, *13*, 308–311.

28 Trewyn, B. G.; Slowing, I. I.; Giri, S.; Chen, H.-T.; Lin, V. S. Y. Synthesis and functionalization of a mesoporous silica nanoparticle based on the sol—gel process and applications in controlled release. *Acc. Chem. Res.* **2007**, *40*, 846–853.

29 Ambrogio, M. W.; Thomas, C. R.; Zhao, Y.-L.; Zink, J. I.; Stoddart, J. F. Mechanized silica nanoparticles: A new frontier in theranostic nanomedicine. *Acc. Chem. Res.* **2011**, *44*, 903–913.

30 Li, Z.; Barnes, J. C.; Bosoy, A.; Stoddart, J. F.; Zink, J. I. Mesoporous silica nanoparticles in biomedical applications. *Chem. Soc. Rev.* **2012**, *41*, 2590–2605.

31 Angelos, S.; Yang, Y.-W.; Khashab, N. M.; Stoddart, J. F.; Zink, J. I. Dual-controlled nanoparticles exhibiting AND logic. *J. Am. Chem. Soc.* **2009**, *131*, 11344–11346.

32 Meng, H.; Xue, M.; Xia, T.; Zhao, Y.-L.; Tamanoi, F.; Stoddart, J. F.; Zink, J. I.; Nel, A. E. Autonomous in vitro anticancer drug release from mesoporous silica nanoparticles by pH-sensitive nanovalves. *J. Am. Chem. Soc.* **2010**, *132*, 12690–12697.

33 Nel, A. E.; Madler, L.; Velegol, D.; Xia, T.; Hoek, E. M. V.; Somasundaran, P.; Klaessig, F.; Castranova, V.; Thompson, M. Understanding biophysicochemical interactions at the nano-bio interface. *Nat. Mater.* **2009**, *8*, 543–557.

34 Castranova, V.; Vallyathan, V. Silicosis and coal workers' pneumoconiosis. *Environ. Health Perspect.* **2000**, *108*, 675–684.

35 Donaldson, K.; Borm, P. J. A. The quartz hazard: A variable entity. *Ann. Occup. Hyg.* **1998**, *42*, 287–294.

36 Elias, Z.; Poirot, O.; DaniÃre, M. C.; Terzetti, F.; Marande, A. M.; Dzwigaj, S.; Pezerat, H.; Fenoglio, I.; Fubini, B. Cytotoxic and transforming effects of silica particles with different surface properties in Syrian hamster embryo (SHE) cells. *Toxicol. In Vitro* **2000**, *14*, 409–422.

37 Rimal, B.; Greenberg, A. K.; Rom, W. N. Basic pathogenetic mechanisms in silicosis: Current understanding. *Curr. Opin. Pulm. Med.* **2005**, *11*, 169–173.

38 Zhuravlev, L. T. Concentration of hydroxyl groups on the surface of amorphous silicas. *Langmuir* **1987**, *3*, 316–318.

39 Zhang, H.; Dunphy, D. R.; Jiang, X.; Meng, H.; Sun, B.; Tarn, D.; Xue, M.; Wang, X.; Lin, S.; Ji, Z.; Li, R.; Garcia, F. L.; Yang, J.; Kirk, M. L.; Xia, T.; Zink, J. I.; Nel, A.; Brinker, C. J. Processing pathway dependence of amorphous silica nanoparticle toxicity: Colloidal vs. pyrolytic. *J. Am. Chem. Soc.* **2012**, *134*, 15790–15804.

40 Fubini, B.; Fenoglio, I.; Elias, Z.; Poirot, O. Variability of biological responses to silicas: Effect of origin, crystallinity, and state of surface on generation of reactive oxygen species and morphological transformation of mammalian cells. *J. Environ. Pathol., Toxicol. Oncol.* **2001**, *20*, 109–118.

41 Hudson, S. P.; Padera, R. F.; Langer, R.; Kohane, D. S. The biocompatibility of mesoporous silicates. *Biomaterials* **2008**, *29*, 4045–4055.

42 Yu, T.; Malugin, A.; Ghandehari, H. Impact of silica nanoparticle design on cellular toxicity and hemolytic activity. *ACS Nano* **2011**, *5*, 5717–5728.

43 Slowing, I. I.; Wu, C.-W.; Vivero-Escoto, J. L.; Lin, V. S. Y. Mesoporous silica nanoparticles for reducing hemolytic activity towards mammalian red blood cells. *Small* **2009**, *5*, 57–62.

44 Nash, T.; Allison, A. C.; Harington, J. S. Physico-chemical properties of silica in relation to its toxicity. *Nature* **1966**, *210*, 259–261.

45 Schoonen, M. A. A.; Cohn, C. A.; Roemer, E.; Laffers, R.; Simon, S. R.; O'Riordan, T. Mineral-induced formation of reactive oxygen species. *Rev. Mineral. Geochem.* **2006**, *64*, 179–221.

46 Ghiazza, M.; Polimeni, M.; Fenoglio, I.; Gazzano, E.; Ghigo, D.; Fubini, B. Does vitreous silica contradict the toxicity of the crystalline silica paradigm? *Chem. Res. Toxicol.* **2010**, *23*, 620–629.

47 Brinker, C. J.; Kirkpatrick, R. J.; Tallant, D. R.; Bunker, B. C.; Montez, B. NMR confirmation of strained defects in amorphous silica. *J. Non-Cryst. Solids* **1988**, *99*, 418–428.

48 Griscom, D. L.; Brinker, C. J.; Ashley, C. S. Electron-spin-resonance studies of irradiated O-17-enriched sol-gel silicas - organic impurity effects and the structure of the nonbridging-oxygen hole center. *J. Non-Cryst. Solids* **1987**, *92*, 295–301.

49 He, Q.; Zhang, Z.; Gao, Y.; Shi, J.; Li, Y. Intracellular localization and cytotoxicity of spherical mesoporous silica nano-and microparticles. *Small* **2009**, *23*, 2722–2729.

50 Meng, H.; Yang, S.; Li, Z.; Xia, T.; Chen, J.; Ji, Z.; Zhang, H.; Wang, X.; Lin, S.; Huang, C.; Zhou, Z. H.; Zink, J. I.; Nel, A. E. Aspect ratio determines the quantity of mesoporous silica nanoparticle uptake by a small GTPase-dependent macropinocytosis mechanism. *ACS Nano* **2011**, *5*, 4434–4447.

51 Malvindi, M. A.; Brunetti, V.; Vecchio, G.; Galeone, A.; Cingolani, R.; Pompa, P. P. SiO$_2$ nanoparticles biocompatibility and their potential for gene delivery and silencing. *Nanoscale* **2012**, *4*, 486–495.

52 Hu, C.-M. J.; Zhang, L.; Aryal, S.; Cheung, C.; Fang, R. H.; Zhang, L. Erythrocyte membrane-camouflaged polymeric nanoparticles as a biomimetic delivery platform. *Proc. Natl. Acad. Sci. U.S.A.* **2011**, *108*, 10980–10985.